IFAC-PapersOnLine, Vol. 49, Issue 11, 2016, pp. 265-270
DOI:10.1016/j.ifacol.2016.08.040

Regularized MPC for Power Management of Hybrid Energy Storage Systems with Applications in Electric Vehicles ⋆

Théo Amy * **He Kong** * **Daniel Auger** * **Gregory Offer** ** **Stefano Longo** *

* *Centre for Automotive Engineering and Technology, Cranfield University, United Kingdom. (email: {t.a.amy, h.kong, d.j.auger, s.longo}@cranfield.ac.uk)*
** *Department of Mechanical Engineering, Imperial College, London (e-mail: gregory.offer@imperial.ac.uk)*

Abstract: This paper examines the application of Regularized Model Predictive Control (RMPC) for Power Management (PM) of Hybrid Energy Storage Systems (HESSs). To illustrate, we apply the idea to the PM problem of a battery-supercapacitors (SCs) powertrain to reduce battery degradation in Electric Vehicles (EVs). While the application of Quadratic MPC (QMPC) in PM of HESS is not new, the idea to examine RMPC here is motivated by its capabilities to prioritize actuator actions and efficiently allocate control effort, as advocated by recent works in the control and MPC literature. Thorough simulations have been run over standard urban test drive cycles. It is found out that QMPC and RMPC, compared to rule-based PM strategies, could reduce the battery degradation over 70%. It is also shown that RMPC can slightly outperform QMPC in reducing battery degradation. Moreover, RMPC, compared to QMPC, could potentially extend the range of that SCs can be used, thus exploiting the degree of freedom of the powertrain to a larger extent. We also make some discussions on the feasibility issues and tuning challenges that RMPC faces, among others.

Keywords: Model Predictive Control, Electric Vehicles, Power Management, Hybrid Energy Storage Systems

1. INTRODUCTION

Despite the rigorous development of electric vehicles and battery techniques (see, Gao et al. (2015), Howey et al. (2014)), battery degradation remains as an chanllenging issue due to high temperature, low and high state of charge (SoC), etc, Wu et al. (2015). An intuitive idea to reduce degradation is to combine various types of energy storage systems in the powertrain Ehsani et al. (2009). Especially, SCs have the capabilities to deliver highly fluctuating power demand and restore regenerating power efficiently, with nearly negligible degradation to themselves. However, the benefits of building a Battery-SCs EV powertrain also come along with several challenges. On the one hand, careful consideration has to be taken regarding the topology of the powertrain. Numerous topologies have been proposed, including passive, semi-active, and active hybrid topologies Aharon and Kuperman (2011). In this paper, we choose the active hybrid topology given the design and control freedom and the energy efficiency that it offers at the expense of a more complicated DC/DC converter setup. In particular, we assume that the parallel active hybrid topology is applied and two DC/DC converters are plugged in parallel from the battery and the SCs terminals to the load, respectively. A major advantage of this topology is that it alleviates the problem of SC voltage variations and allows a nearly constant current flow from the battery.

Another challenge is the design of PM strategies. Many techniques can be used to control the power split between batteries and SCs, including heuristic, static, and dynamic optimisation strategies Sun (2015). Although heuristic and rule-based methods are computationally efficient and easy to implement, they often incur a lot of trial and error and do not determine the optimal power split because they do not take into account the trajectory of an EV journey. Therefore, several optimization-based strategies have been proposed in the literature. Static optimisation strategies are based on optimal control theory and aim to minimize a cost function to obtain the optimal power split. However, the vehicle path needs to be known entirely and it is optimal only over a certain vehicle path. On the contrary, dynamic optimisation strategies combine an estimation of the future power demand and an online optimisation problem to determine the optimal power split.

Note that battery degradation has important implications on the efficiency of an EV powertrain and should be taken account into the optimization, Auger et al. (2014), Fotouhi et al. (2014). This paper focuses on dynamic optimisation strategies for PM of a battery-SCs powertrain by implementing MPC to minimize battery degradation. We remark that the PM problem can be considered as a

⋆ Supported by the "Developing FUTURE Vehicles" project of the British Engineering and Physical Sciences Research Council.

control allocation question, which has been a topic of interest in the control community for several years Johansen & Fossen (2013). It has been shown in several existing works that QMPC can offer noticeable performance improvements compared to available controllers in the commercial powertrain system analysis toolkit, Santucci et al. (2014), Borhan et al. (2012). Of particular interest here is RMPC, which has been recently proposed and advocated for its capabilities to prioritize actuator actions and efficiently allocate control effort, Ohlsson et al. (2010), Gallieri & Maciejowski (2012), Pakazad et al. (2013), Aguilera et al. (2014). RMPC is different from QMPC in its cost formulation by featuring a regularization term in addition to the quadratic part. This extra term can be tuned to penalize control actions of different actuators. RMPC is also pertinent to the topics of sparse communication and control in networked control Nagahara et al. (2014), Kong et al. (2015). Motivated by the above theoretical development in RMPC, we aim to examine the application of RMPC to PM of a battery-SC powertrain. We will show that for low speed profiles such as Artemis Urban Drive Cycle (AUDC), RMPC can slightly outperform QMPC in reducing battery degradation. Moreover, RMPC, compared to QMPC, could potentially make better use of the SCs, thus exploiting the degree of freedom of the powertrain to a larger extent.

2. SIMULATION MODELING

2.1 Vehicle dynamics

To simulate the vehicle's behaviour, forces applied to the vehicle are modelled to derive the power demand required from the drive cycle as a function of time. To simplify, three main forces are considered. The first force is the aerodynamic drag modelled as $R_a = \frac{1}{2}\rho c_d A v^2$, where ρ is the air density, A, c_d, and v are the frontal area, the drag coefficient and the speed of the vehicle, respectively. The second force is the rolling resistance $R_r = Mgf$, where M is the mass of the vehicle, g is the acceleration due to the gravity and f is the coefficient of rolling resistance. The third force is the inertia resistance during longitudinal motions $R_i = Ma$, where M and a are the mass and the acceleration of the vehicle, respectively. Eventually, the expected power demand from the driver is $P = (R_a + R_r + R_i)v$. The parameters in the simulations are based on the Nissan Leaf specifications Nissan (2015).

2.2 Battery model

The battery model used is a Thévenin model as represented in Figure 1, where R_0 and C are the internal resistance

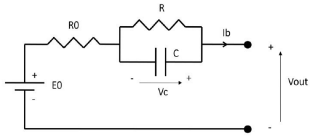

Fig. 1. Thévenin model of a battery

and capacitance (both assumed to be constant), respectively; R is the overvoltage resistance; V_C is the voltage across the capacitor and the ideal voltage is E_0. Based on Kirchhoff's laws, the following equations are derived involving P_b as the power of the battery:

$$\begin{aligned} \dot{V_C} &= -\frac{V_C}{RC} + \frac{i_b}{C}, \\ V_C &= \frac{E_0 + V_C + \sqrt{(E_0+V_C)^2 - 4R_0P_b}}{2} \\ i_b &= \frac{2P_{batt}}{E_0 + V_C + \sqrt{(E_0+V_C)^2 - 4R_0P_b}}. \end{aligned} \tag{1}$$

Following Auger et al. (2014), we have $\dot{SoC_b} = \frac{i_b}{3600k_c}$, where k_c is the battery capacity (in Ah) and i_b is defined in (1). The factor of 3600 converts from [Ah] to equivalent base International System (SI) of units. Moreover, as in Auger et al. (2014), we use a constant capacity k_c to maintain simplicity. We then have the battery model:

$$\dot{SoC_b} = \frac{i_b}{3600k_c},\ \dot{V_C} = -\frac{V_C}{RC} + \frac{i_b}{C}. \tag{2}$$

The battery degradation model considered here takes into account the current and the current rate of the battery:

$$E = \int_0^{t_f} \frac{|i_b|}{7200k_cN_{cycle}}dt + \int_0^{t_f} \frac{\dot{i_b}}{KC_rt_f}dt \tag{3}$$

where t_f is the simulation final time; N_{cycle} is extracted from the battery properties and provided by the manufacturer; K is a ratio between the current and the current rate, C_r is the average current rate over a drive cycle.

Remark 1. The degradation criteria (3) is in close spirit to that of Serrao et al. (2014) and Santucci et al. (2014). We remark that it is reasonable to assume that SoC_b does not affect degradation as long as we prevent SoC_b from going very high or very low (in the simulations, we keep it between $10\% \sim 90\%$). We also assume that the battery management system can control the battery pack's temperature perfectly, i.e., the impact of the temperature on battery degradation is not considered and it is the high current excursions and high rates of change of current that generate significant amounts of degradation. High currents can also generate stresses within electrode particles causing them to fracture and break. Many other degradation mechanisms happen too. Therefore, such assumptions are not realistic in practice and generalizations of the proposed results to consider more practical scenarios are possible and are part of our future work.

2.3 SC model

The SC model used is described in Figure 2, where

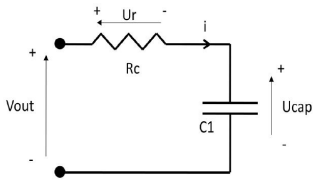

Fig. 2. Equivalent circuit representation of a SC

V_{out} is the voltage delivered by the SC; U_{cap} is the voltage across the capacitor C_1; R_C and C_1 are the internal resistance and capacitance, respectively Ehsani et al. (2009). Following similar steps in deriving the battery model, the SC model is obtained using P_{sc} as the power delivered by SC:

$$V_{out} = \frac{1}{2}\left[U_{cap} + \sqrt{U_{cap}^2 - 4R_cP_{sc}}\right],$$
$$i = \frac{2P_{sc}}{U_{cap} + \sqrt{U_{cap}^2 - 4R_cP_{sc}}}, \dot{U_{cap}} = -\frac{i}{C_1}. \quad (4)$$

Then, the model of a SC pack can be written as:

$$\dot{U_{cap}} = -\frac{1}{C_{pack}}i \quad (5)$$

where i is defined in (4), $C_{pack} = \frac{np_c}{ns_c}C_{cell}$ and $R_{pack} = \frac{ns_c}{np_c}R_{cell}$ with np_c and ns_c representing the numbers of SCs in parallel and in series, respectively. Based on these formulations and using $U_{cap}^{\max}$, the maximum voltage the SCs can provide, we define the SoC of the SC pack as

$$SoC_{sc} = \frac{U_{cap}}{U_{cap}^{\max}}. \quad (6)$$

The SCs' parameters used in the paper are obtained from Maxwell Technologies (2013).

2.4 DC/DC converter model

Since the efficiency of bi-directional buck boost DC/DC converters is typically around 90 to 95%, we model the DC/DC converters with a constant efficiency equal to 90%, for simplicity and without loss of generality. A schematic overview of the PM problem is illustrated in Figure 3.

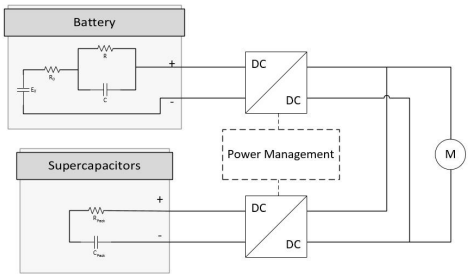

Fig. 3. Schematic overview of the PM problem

2.5 State space representation

Using the models of the battery and SCs developed above, state space formulations of the PM question can be derived. Since the aim of this study is to minimize battery degradation, knowing exactly the battery SoC is not necessary. Therefore, to simplify the model, we assume that V_c in (2) is equal to zero. Then we have the state space representation of the battery-SCs powertrain system as

$$\dot{SoC_b} = \frac{i_b}{3600k_c},\ \dot{U_{cap}} = -\frac{1}{C_{pack}}i, \quad (7)$$

where i_b, i and C_{pack} are defined in (1), (4), (5), respectively. Note that P_b and P_{sc} are two inputs that are to be manipulated in the PM strategies.

3. POWER MANAGEMENT STRATEGIES

3.1 Rule-based strategies

As remarked earlier, rule-based strategies have been widely applied in practice due to its computational efficiency. To better understand the trade-off between different strategies, two simple rule-based strategies are used as a baseline for comparison in the simulations of this paper (see in Section 5 for more details).

3.2 Quadratic MPC

We next present some preliminaries of the MPC theory for linear systems. Consider the LTI discrete-time model:

$$x_{k+1} = Ax_k + Bu_k \quad (8)$$

where $x_k \in \mathbf{R}^n$, $u_k \in \mathbf{R}^m$ are the state and the input, respectively. When MPC is applied for system (8), the desired performance is usually captured by a cost function of the following form:

$$V = \sum_{t=0}^{N-1}[x_{k+t}^{\mathrm{T}}Qx_{k+t} + u_{k+t}^{\mathrm{T}}R_su_{k+t}] + x_{k+N}^{\mathrm{T}}Px_{k+N}, \quad (9)$$

where

$$\begin{cases} x_k = x,\ x_{k+t} \in \mathbf{X}, \text{ for } t = 0, \dots N \\ u_{k+t} \in \mathbf{U}, \text{ for } t = 0, \dots N-1 \end{cases}. \quad (10)$$

In (10), the sets $\mathbf{U}$ and $\mathbf{X}$ are appropriate sets that capture the constraints that the system is required to satisfy; the vector x_{k+t} represents the prediction of the state vector of the system at time $k+t$ based on the model in (8) and the state information $x_k = x$ available at time k. The weighting matrices satisfy $Q \geq 0, R_s > 0$ whilst the terminal weighting matrix P is usually taken to be the unique symmetric positive definite solution to the discrete time algebraic Riccati equation Kong et al. (2012). MPC solves, at each time step, the optimization problem and only applies the first m elements of the optimal control vector to the system (8). The optimization procedure is repeated when a new state estimate becomes available. For more detailed discussions on MPC, one can refer to Goodwin et al. (2005), Goodwin et al. (2014), Maciejowski (2002), Kong et al. (2013).

3.3 Regularized MPC

Regularised MPC differs from QMPC in that it adds a regularized term to the quadratic cost terms in (9):

$$J = \sum_{t=0}^{N-1}[x_{k+t}^{\mathrm{T}}Qx_{k+t} + u_{k+t}^{\mathrm{T}}R_su_{k+t} + \lambda\left|u_{k+t}\right|_1] + x_{k+N}^{\mathrm{T}}Px_{k+N}$$

where, $\lambda\left|u_{k+t}\right|_1$ is the regularization term, with $\left|u_{k+t}\right|_1$ representing the ℓ_1 norm of the vector u_{k+t}, and λ is a parameter with positive values. The regularization term can be considered as a penalization mechanism to coordinate and prioritize the control input in the actuators. Note that the tuning of λ, together with the weighting matrices Q, R_s, P, affects closed-loop stability and performance, and is in general a non-trivial issue. For more discussions on the tuning of λ, we refer the reader to Ohlsson et al. (2010), Gallieri & Maciejowski (2012), Kim et al. (2008), Aguilera et al. (2014). Quite often (but not necessarily), when the value of λ is increased, more elements in the control vector tend to be zeros. Thus, RMPC can reduce or prioritize actuator activities by exploiting the degree of freedom in selecting the regularization term.

An important observation to be noted from the model (7) is that in the PM question of a battery-SCs powertrain, the

two power sources can be considered as 'actuators' with P_b and P_{sc} are their control inputs. To minimize battery degradation, it is preferred that P_b changes smoothly and P_{sc} deals with the fast changes in the power demand. By doing so, the current going through the battery will change smoothly since we assume that the DC/DC converter works efficiently. Thus, it naturally leads us to examine the application of the RMPC in PM of HESS.

4. SIMULATION SETUP AND RESULTS

4.1 System model and cost functions

We adopt the nonlinear state-space model (7) for the purpose of simulation. As noted in Remark 1, the impact of the temperature on the battery degradation is not considered here. Based on this simplifying assumption, we choose the current and the current rate going through the battery as measures of battery degradation. To this end, a quadratic cost function is developed first to penalize the current and the derivative of the current as follows:

$$J_Q = qP_b^2 + r\frac{1}{P_{sc}^2} \tag{11}$$

where q and r are tuning parameters with positive values. Based on (11), the cost function for RMPC is proposed

$$J_R = qP_b^2 + r\frac{1}{P_{sc}^2} + \lambda\left|P_b\right|_1 \tag{12}$$

where $\lambda\left|P_b\right|_1$ is introduced to regularize the power delivered by the battery; λ is a positive parameter to be tuned. In principle both J_Q and J_R can penalize the input to be small. But we include $\lambda\left|P_b\right|_1$ in J_R to potentially have more degree of freedom in allocating power between P_b and P_{sc}, as motivated by the works in Gallieri & Maciejowski (2012), Gallieri & Maciejowski (2015). We remark that J_Q and J_R are used in the optimization as stage costs.

4.2 System constraints

Based on the battery and SC models and the consideration that energy can be transferred between the two power sources, we define the constraints of the system as below:

$$\begin{cases} SoC_b \in [0.1, 0.9]\,,\ SoC_{sc} \in [0.25, 1]\,, \\ P_b < \dfrac{(E_0+V_c)^2}{4R_0}, P_{sc} < \dfrac{U_{cap}^2}{4R_{pack}}, P_d = P_b + P_{sc}, \\ 0.5U_{sc} < U_{sc} < U_{sc}^{\max}, P_b \in \left[-P_{reg}^{\max}, P_{prov}^{\max}\right]. \end{cases} \tag{13}$$

where $P_{reg}^{\max}$ is the maximum power rate at which the battery could be recharged and $P_{prov}^{\max}$ is the maximum power that can be provided by the battery to prevent damages; based on (6) and the desired working range of the Scs, the constraint over U_{sc} is derived; the constraints over P_b and P_{sc} are derived to keep the power values in the real domain, based on (1) and (4), respectively. It should be noted that in (13), the constraint $P_d = P_b + P_{sc}$ is enforced in the optimization to maintain the drivability of the vehicle. This has important implications in assessing the appropriateness of RMPC in the PM problem, which is to be discussed in the next section.

4.3 Simulation results

Using the setup made above, simulations are run over different drive cycles using the optimization toolbox ICLOCS Falugi et al. (2010). The prediction horizon is selected to be $500s$, i.e., the drive cycle is assumed to be known $500s$ ahead. At each sampling instant, the input in the prediction window of $100s$ in the resultant optimal input sequence is applied. The same procedure is repeated at next sampling instant. Note that we choose the horizons to be relatively longer than what is usually required in practice to have a better understanding of the potential advantages and limitations of optimization-based strategies. Future work will explore the choices of shorter horizons. Simulations are mainly run over AUDC. The results are illustrated in Figure 4-6, where the black dotted line, the red dash dotted line, the purple solid line and the green dashed line represent the battery current when the following techniques are applied, respectively: rule based strategy using battery only (RBBO), rule based strategy using battery with SCs (RBBSC), QMPC and RMPC. For the RBBO strategy, all the power is provided by the battery. For the RBBSC strategy, if the SoC of the SC pack is higher than 25%, then SC pack provides all the power; if the SC pack's SoC is lower than 25 %, the battery provides all the power. The following observations can be made from Figure 4:

(a) Without including SCs into the power train, there are a lot of overshoots in the current profile of RBBO since the battery has to be charged or discharged to meet the power demand. Note that such overshoots can cause serious degradation to the battery. When SCs are included into the rule-based strategy, the SCs have been used to absorb the regenerative power. This is reflected in Figure 4 that the battery current is zero or negative during the simulation time. Moreover, it can be checked that using RBBSC, the average current delivered by the battery becomes to $4.8A$ while it is equal to $8.6A$ using RBBO. Similarly, the average current change rate has been reduced by 2.35 times using RBBSC, compared to RBBO.

(b) For the battery-SCs power train, with QMPC, the current profiles of the battery appear to be much smoother than those of RBBO and RBBSC. It can be seen that the current delivered by the battery remains close to (but not) zero. This will reduce the degradation significantly, compared to the rule based strategies. Similarly with QMPC, RMPC can reduce the overshoot in the current profiles, compared to rule based techniques. In fact, it can be seen that the current profiles of QMPC and RMPC are very close to each other. Moreover, one can also observe that there are more moderate fluctuations in the current profile of RMPC, compared to QMPC. However, it is also observed that there are more times in the current profile of RMPC when the current is closer to zero than that of QMPC. Actually, similar phenomena have been experienced in the simulation examples of Gallieri & Maciejowski (2012). In fact, such phenomena are expected outcomes of applying RMPC. The reason is RMPC tries to minimize the utilization of the penalized input in the regularized term, apart from the quadratic terms. In our case, we aim to attenuate the power delivered by the battery so that the current going through is smooth. Consequently, RMPC tries to bring the battery power to zero as often as possible. Nonetheless, the power demand from the driver is changing over AUDC. To maintain the driveability of the vehicle, if the power from SCs cannot meet the driver demand, a certain amount of

power shall be drawn from the battery. This explains more (but moderate) fluctuations as experienced in the current profile of RMPC, as compared to QMPC.

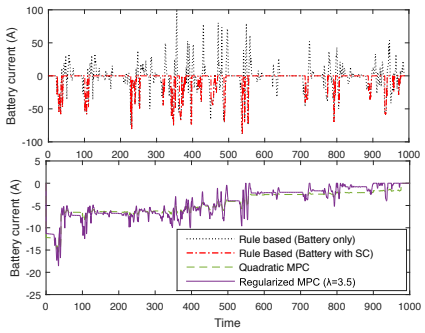

Fig. 4. Battery current with different strategies

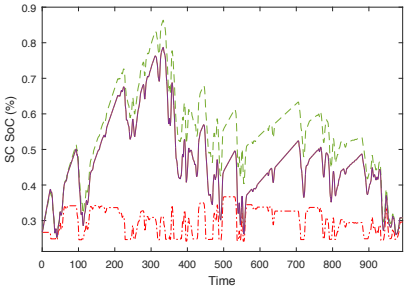

Fig. 5. SoC of the SC pack with different strategies

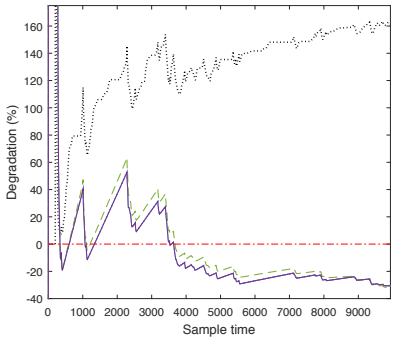

Fig. 6. Degradation by different PM strategies

The SoC of the SCs for different strategies are presented in Figure 5. It can be seen from Figure 5 that using RBBSC, the SoC remains between 25% and 37% because the strategy is built to use power from the SC pack whenever its SoC is higher than 25%. Using QMPC, the utilisation of the SCs is considerably increased and the SoC varies between 25% and 80.9%. In the meantime, RMPC outperforms QMPC by increasing the SoC range of SC to about 87.7%. This is not unexpected, since RMPC aims to penalize the power going through the battery whenever possible and extra power will eventually go to the SCs. Thus, it can be concluded that RMPC can utilize the SCs to a larger extent, thereby further exploiting the degree of freedom in the battery-SCs powertrain. Although we have assumed SCs do not degrade, in practice they do. However, they are rated for millions of charge/discharge cycles and their impedance is significantly lower than batteries. If degradation is assumed to be proportional to heat generation, shifting energy throughput into the SCs rather than the batteries, should reduce net degradation of the two components. Thus, extending the range of the utilisation of the SCs could help to reduce net degradation.

Finally, we plot Figure 6 to compare the battery degradation using the different strategies. Note that the real value of the degradation is a value that is changing with time. To better illustrate the results, we take the value of battery degradation using RBBSC as a comparison reference valued at zero. The values of the battery degradation using other strategies are compared against that of RBBSC. It can be seen from Figure 6 that compared to RBBSC the degradation at the beginning of the drive cycle is more aggressive using QMPC and RMPC. A reason is that at the beginning of the driver cycle, both QMPC and RMPC will tend to discharge the battery to meet the driver demand and recharge the SCs, thereby inducing a current rate which is not necessarily smoother than that of RBBSC. However, as time proceeds, both QMPC and RMPC incur less severe battery degradation than RBBSC. In fact, at the end of the drive, the battery degradation is reduced by 30.25% and 31.35% using QMPC and RMPC, respectively, compared to RBBSC.

4.4 Discussions and future work

We next present discussions on some aspects of applying RMPC in PM of HESSs. Firstly, from the above simulation results, it can be concluded that RMPC achieves the best results in terms of battery degradation minimisation. It slightly outperforms QMPC at the end of the driver cycle. Moreover, RMPC enables extending the SoC range of the SCs thus better exploit the degree of freedom in the hybrid powertrain. However, it should be noted that RPMC faces certain issues and challenges. For example, RMPC usually necessitates a longer computational time than QMPC. Besides, the tuning of the regularization parameter λ is not intuitive. The tuning of this parameter has been long recognized as a challenge, since the value of λ affects the solution of RMPC in a way that is difficult to measure a priori Kim et al. (2008). In fact, we have tried to run the simulation over high speed profiles such as Artemis Rural and Motorway Drive Cycles. Due to limited space, the results are not included here. What we have found out from these simulations is that at the end of the drive cycles, RMPC achieves almost the same results with QMPC in minimizing battery degradation. However, there are more aggressive fluctuations in the battery current profile using RMPC than the case using QMPC. For these high speed profile drive cycles, tuning λ only bring minor changes to the simulation results. The main reason for this is that for the PM problem at hand, the two inputs, i.e., P_b and P_{sc}, are actually coupled by the driver demand equality constraint in (13). This requirement brings a fundamental limitation on the outcome that RMPC can achieve. Indeed,

in this application, with the two inputs being coupled, there is only one degree of freedom in the optimization. When the designer chooses to regularize one input using RMPC, the other one is indirectly affected. Therefore, we believe RMPC, compared to QMPC, could offer certain extra benefits, for low speed drive cycles, at the expense of a larger computation burden. Despite that, it also faces tuning challenges and feasibility issues as explained above. Our conjecture is that the feasibility limitations can be better dealt with for HESSs with more degrees of freedom, i.e., three or more types of power sources (e.g., a powertrain consisting fuel cells, batteries and SCs). Extension to such scenarios are topics of interest for future work. It will also be interesting to run RMPC in hardware-in-the-loop test benches to better understand the potential and computational limitations of the method.

5. CONCLUSION

This paper has examined the application of RMPC to PM of a battery-SCs powertrain in EVs. Based on some simplifying assumptions on the battery and SC models, we have compared RMPC against QMPC and rule-based strategies in terms of battery degradation minimisation. It can be concluded from the simulations run over AUDC that RMPC brings the benefits of extending the utilization range of the SCs while also slightly outperforming QMPC in reducing battery degradation. We also point out some topics for future research.

REFERENCES

Aguilera, R. P., Delgado R., Dolz, D. & Aguero, J. C. (2014). Quadratic MPC with ℓ_0-input constraint. *Proc. of the 19th IFAC World Congress,* pp. 10888-10893.

Aharon, I. & Kuperman, A. (2011). Topological overview of powertrains for battery-powered vehicles with range extenders. *IEEE Trans. on PE*, Vol. 26, No. 3, pp. 868-876.

Auger, D. J., Groff, M. F., Mohan, G., Longo, S., & Assadian, F. (2014). Impact of Battery Ageing on an Electric Vehicle Powertrain Optimisation. *Journal of Sustainable Development of Energy, Water and Environment Systems*, Vol. 2, No. 4, pp. 350-361.

Borhan, H., Vahidi, A., Phillips, A., Kuang, M. L., Kolmanovsky, I., & Cairano, S. D. (2012). MPC-based energy management of a power-split hybrid electric vehicle. *IEEE Trans. on CST*, Vol. 20, No. 3, pp. 593–603.

Fotouhi, A., Auger, D. J., Propp, K. & Longo, S. (2014). Simulation for prediction of vehicle efficiency, performance, range and lifetime: a review of current techniques and their applicability to current and future testing standards. *Proc. of 5th IET HEVC*, London.

Ehsani, M., Gao, Y., & Emadi, A. (2009). Modern electric, hybrid electric, and fuel cell vehicles: fundamentals, theory, and design. CRC Press.

Falugi, P., Kerrigan, E., & Wyk, E. (2010). Imperial college london optimal control software user guide (ICLOCS). http://www.ee.ic.ac.uk/ICLOCS/

Gallieri, M. & Maciejowski, J. M. (2012). The ℓ_{asso} MPC: smart regulation of over-actuated systems. *Proc. of the ACC*, pp. 1217-1222, Montreal, Canada.

Gallieri, M. & Maciejowski, J. M. (2015). Model predictive control with prioritised actuators. *Proc. of the ECC*, pp. 533-538, Linz, Austria.

Gao, B., Xiang, Y., Chen, H., Liang, Q., & Guo, L. (2015). Optimal trajectory planning of motor torque and clutch slip speed for gear shift of a two-speed electric vehicle. *ASME Journal of DSMC*, Vol. 137, No. 6, pp. 1-9.

Goodwin, G. C., Seron, M. M. & Dona, J. D. (2005). Constrained control and estimation: an optimization approach. New York: Springer.

Goodwin, G. C., Kong, H., Mirzaeva, G., & Seron, M. M. (2014). Robust model predictive control: reflections and opportunities. *Journal of Control and Decision*, Vol. 1, No. 2, pp. 115-148.

Howey, D. A., Mitcheson, P. D., Yufit, V., Offer, G., & Brandon, N.P. (2014). Online measurement of battery impedance using motor controller excitation. *IEEE Trans. on VT*, Vol. 63, No. 6, pp. 2557-2566.

Johansen, T. A. & Fossen, T. I. (2013). Control allocation–a survey. *Automatica*, Vol. 49, No. 5, pp. 1087-1103.

Kim, S. J., Koh, K., Lustig, M., Boyd, S., & Gorinevsky, D. (2008). An interior-point method for large-scale ℓ_1-regularized least squares. *IEEE Journal of Selected Topics in SP*, Vol. 1, No. 4, pp. pp. 606-617.

Kong, H., Goodwin, G. C., & Seron, M. M. (2015). A cost-effective sparse communication strategy for networked linear control systems: an SVD-based approach. *Int. Journal of RNC*, Vol. 25, No. 14, pp. 2223–2240, 2015.

Kong, H., Goodwin, G. C., & Seron, M. M. (2013). Predictive metamorphic control. *Automatica*, Vol. 49, No. 12, pp. 3670-3676.

Kong, H., Goodwin, G. C., & Seron, M. M. (2012). A revisit to inverse optimality of linear systems. *Int. Journal of Control*, Vol. 85, No. 10, pp. 1506-1514.

Maciejowski, J. M. (2002). Predictive control with constraints. Harlow, UK.: Prentice-Hall/Pearson.

Maxwell Technologies. (2013). Datasheets. http://www.datasheetarchive.com/dl/Datasheets-IS36/DSA00713317.pdf [Accessed 10 April 2015].

Nagahara, M., Quevedo, D. E., & Ostergaard, J. (2014). Sparse packetized predictive control for networked control over erasure channels. *IEEE Trans. on Automatic Control*, Vol. 59, No. 7, pp. 1899-1905.

Nissan (2015). Nissan LEAF: the new car, 100% electric, no gas, features & specifications. Available online.

Ohlsson, H., Gustafsson, F., Ljung, L., & Boyd, S. (2010). Trajectory generation using sum-of-norms regularization. *Proc. of IEEE CDC*, pp. 540-545, Atlanta, GA.

Pakazad, S. K., Ohlsson, H. & Ljung, L. (2013). Sparse control using sum-of-norms regularized model predictive control. *Proc. of IEEE CDC*, pp. 5758-5763, Florence.

Santucci, A., Sorniotti, A. & Lekakou, C. (2014). Power split strategies for hybrid energy storage systems for vehicular applications. *Journal of PS*, Vol. 258, pp. 395-407.

Serrao, L., Onori, S., Sciarretta, A., Guezennec, Y. & Rizzoni, G. (2011). Optimal energy management of hybrid electric vehicles including battery aging. *Proc. of the ACC*, pp. 2125-2130, San Francisco, CA.

Sun, J. (2015). Optimisation-based control for electrified vehicles: challenges and opportunities. *Journal of Control and Decision*, Vol. 2, No. 1, pp. 46-63.

Wu, B., Yufit, V., Merla, Y, Martinez-Botas, R. , Brandon, N. & Offer, G. (2015). Differential thermal voltammetry for tracking of degradation in lithium-ion batteries. *Journal of PS*, Vol. 273, pp. 495-501.

2016-08-21

Regularized MPC for power management of hybrid energy storage systems with applications in electric vehicles

Amy, T.

Elsevier

Amy T, Kong H, Auger D, Offer G, Longo S, Regularized MPC for Power Management of Hybrid Energy Storage Systems with Applications in Electric Vehicles, IFAC-PapersOnLine, Volume þÿ4 9 , I s s u e 1 1 , 2 0 1 6 , P a g e s 2 6 5 2 7 0 .

http://dx.doi.org/10.1016/j.ifacol.2016.08.040